

Fabrication of Flexible Transparent Conductive Coatings Based on Single-Walled Carbon Nanotubes

K. F. Akhmadishina, I. I. Bobrinetskii, R. A. Ibragimov, I. A. Komarov, A. M. Malovichko, V. K. Nevolin, and V. A. Petukhov

MIET National Research University of Electronic Technology, proezd 4806 5, Zelenograd, Moscow, 124498 Russia

e-mail: vkn@nanotube.ru

Received June 11, 2013

Abstract—We have proposed a method for large-scale growth of thin nanotube films from solution on the surface of flexible, transparent substrates. Uniform nanotube deposition was achieved through the preparation of a stable colloidal nanotube solution in an aqueous surfactant solution. We examined the effect of the number of deposition cycles on the morphology of the films and their optical and electrical characteristics. The results demonstrate that the optical transmittance of the films decreases linearly with increasing film thickness, whereas their resistance decreases quadratically, which corresponds to three-dimensional nanotube percolation in the films. With increasing film thickness, the sheet resistance of the films drops from 400 to 15 k Ω/\square and their transmittance decreases from 85 to 40%, respectively.

DOI: 10.1134/S0020168514010014

INTRODUCTION

Transparent electrodes are necessary components of many modern devices, such as touch screens, liquid crystal displays, flexible displays, organic light emitting diodes, and solar cells. Such electrodes are commonly produced through vacuum sputtering of conductive oxides, the most widespread of which is indium tin oxide (ITO). Unfortunately, ITO has a number of drawbacks: low mechanical strength, low production yield, high reflectivity, high cost, and the use of complex and environmentally hazardous chemical processes in ITO preparation.

At present, research effort is aimed primarily at creating transparent conductive films (TCFs) from carbon nanomaterials, in particular from carbon nanotubes (CNTs) [1–3]. Most existing approaches involve the preparation of an aqueous CNT solution with surfactants [4] or a CNT solution in alcohols [5]. It is an aqueous nanotube solution with surfactant additions that has been used in most studies. The role of the surfactants is to separate the nanotubes from each other: the surfactants prevent nanotube coagulation and agglomeration—which allows the solution to remain homogeneous for many weeks—with no effect on the electrical properties of the nanotubes. Various surfactants can be used for this purpose, for example, ionic (cetyltrimethylammonium bromide (CTAB), sodium dodecyl sulfate) [6] or nonionic (deoxyribonucleic acid, bovine serum albumin) [7].

The nature of the substrate has a rather significant effect on the film preparation process. In some instances, the substrate should be functionalized [8]; in others, it must withstand high temperatures, up to

600–800°C [9]. The main types of substrate materials commonly used in producing conductive transparent coatings are glass, polycarbonate, polyethylene terephthalate, and polyethylene. Since the main advantage of nanotubes is that they can be used on flexible carriers, it is of interest to study the properties of such films on carriers under mechanical stress. According to such studies, the conductance of the structures in question is generally stable, with deviations within 10% at bend radii of down to 1.5 mm [10] in up to several thousand bending/unbending cycles [11].

A major unresolved problem is optimization of the deposition process, which involves the development of basic mechanisms that would ensure the best transmission/conductance relationship in the films. In this paper, we report an approach to producing thin conductive films from surfactant solutions at temperatures below the critical micelle temperature and describe the electrical properties of such films in relation to the number of constituent layers on the surface of polyethylene naphthalate (PEN) substrates.

EXPERIMENTAL

As flexible substrates, we used 125- μm -thick PEN film (Teijin DuPont Films, Japan) cut into squares 10 \times 10 mm in dimensions. At the edges of the substrates, 100-nm-thick palladium electrodes were deposited by magnetron sputtering (Emitech K575X, Quorum Technologies, UK) through a mask. The electrodes were made after nanotube film growth on the substrate surface.

As a working layer, we used single-walled CNTs (99.5 wt %; provided by A.V. Krestinin, Institute of Problems of Chemical Physics, Russian Academy of Sciences) produced by arc discharge [12]. The single-walled CNTs were added (0.02 mg/mL) to a 0.5% solution of CTAB (Helicon, Russia) and dispersed in a Branson B300 ultrasonically agitated bath (Branson Ultrasonics, USA) for 24 h in order to produce a colloidal solution at a temperature of $\approx 5^\circ\text{C}$ (below the critical micelle temperature of CTAB). The presence of the surfactant and the long dispersion time were needed to obtain single nanotubes—or, at least, bundles as small as possible—in solution. According to atomic force microscopy (AFM) data (Solver Pro instrument, NT-MDT, Russia), the nanotubes were typically less than 1000 nm in length. At the same time, the nanotube length in bundles was up to 5 μm , and the bundle diameter was ≈ 10 nm.

A droplet of the solution was applied to a polymer substrate, spread over the entire surface, and left to dry. Next, the substrate was rinsed in boiling 2-propanol for 5 min to remove the residual surfactant, and the residual solution was evaporated at a temperature below 110–120°C. The process was repeated (5, 10, 15, and 20 times) until the film had the required conductance. In this way, we prepared four series of structures with single-walled CNT films of varied thickness.

The transmittance of the films was measured on a PE-5300VI spectrophotometer (OOO Ekokhim, Russia). Raman spectra were obtained on a Centaur U HR confocal microscope/spectrometer (Nano Scan Technology Ltd.).

The effect of bending on the electrical properties of the films was studied using a home-built programmable system which included a substrate holder. One side of the holder was secured in a support stand, and the other was connected to a servo actuator, which ensured torsion of the free substrate edge. The system makes it possible to set the range of torsion angles and the number of bending cycles in measurements and allows the torsion angle and electrical resistance, measured by an external Agilent 34401A digital multimeter (Agilent Technologies, USA), to be stored on a computer. The substrate was clamped at the contacts and subjected to cyclic bending through angles from $+90^\circ$ (compression) to -90° (tension), which corresponded to a minimum radius of curvature of 3.5 mm.

RESULTS AND DISCUSSION

Homogeneity and thickness of the coatings. The TCF growth procedure includes the following steps: surfactant dissolution in water, the addition of CNTs to the aqueous solution of the surfactant, and application of the CNT solution in the surfactant to the surface of polymer film. If the carrier surface is sufficiently hydrophobic, surfactant molecules begin to form a surface monolayer, attaching to the carrier by their hydrophobic groups. In this process, the thickness and quality of the monolayer are determined by

the temperature: the higher the temperature, the smaller is the percentage of surfactant monomers in solution and the larger is the percentage of micelles. To obtain a monomolecular layer, the temperature should be below the critical micelle temperature [13]. In the next step, during solution drying, the CNTs begin to deposit on the surface of the surfactant monolayer to form a network parallel to the carrier. The presence of residual surfactant and the diameter of single-walled CNT bundles were inferred from topographic AFM images of the films after one deposition cycle (one layer) at different temperatures. The diameter of nanotube bundles deposited on the polymer film surface was found to decrease with decreasing temperature. This was accompanied by a decrease in surfactant concentration. Figure 1 shows topographic images of single-walled CNTs deposited from a CTAB solution at a temperature of $\approx 25^\circ\text{C}$ (Fig. 1a) and 5°C (Fig. 1b).

The proposed technique allows one to produce rather thin layers of nanotube bundles and single nanotubes. Nevertheless, the conductance of the monolayer grown in one deposition cycle was below the detection limit of the multimeter (above 200 G Ω). Several deposition cycles are needed to produce a conductive layer. The thickness of the single-walled CNT films was evaluated through AFM scanning of the surface of the structures obtained. The films had the form of percolated, entangled networks containing high concentrations of pores and voids between nanotube yarns, which might contain residual surfactant (Fig. 2). During thin film growth, nanotubes are non-uniformly deposited on the surface, successively filling voids. The film thickness was evaluated as the full width at half maximum of the peak in the surface height distribution extracted from the AFM image, and uncertainty was estimated as the calculated rms deviation from the average. It should also be taken into account that, when the film thickness exceeds 100 nm and all of the voids are filled with nanotubes, the cantilever is physically incapable of penetrating throughout the pore depth, and measurements become inaccurate [14]. Moreover, an increase in film density is accompanied by increased agglomeration of the nanotubes into large bundles and yarns (Figs. 2c, 2d). Because of this, to more accurately determine the thickness of films more than 100 nm thick, the CNT deposit was partially mechanically removed until the PEN surface was exposed, and the resultant surface height profile was examined by AFM.

Figure 3 plots the average film thickness against the number of grown layers. After five deposition cycles, the film was still highly porous and the average film thickness was ≈ 50 nm. Further increasing the number of layers led to a linear increase in film thickness with a factor of 10, up to an average thickness of 200 nm after 20 deposition cycles. The factor 10 means that the average thickness of one layer was 10 nm, which coincides with the diameter of single-walled CNT bundles forming on the substrate surface during deposition from a surfactant solution. With increasing film

thickness, the porosity decreases considerably. Note that, in analyzing AFM images, one should take into account the distortion of the cantilever probe on the surface of three-dimensional objects, which leads to image broadening (with an uncertainty of up to 100 nm), thereby distorting the information about the film porosity. The uncertainty in our film thickness measurements due to the film inhomogeneity was about 30 nm.

Effect of film thickness on the conductance and transmission of the films. The resistance of the grown films was measured by a standard four probe method. This method enables one to obtain reliable data for homogeneous thick films. At high porosity and low density, like in single-walled CNT films consisting of less than five layers, the method suffers from considerable uncertainty. Nevertheless, the values it gives are the upper limit of the possible film resistance and can be used to assess the effect of the number of layers on the conductance of the films.

As seen in Fig. 4, the resistance of the films is a nonlinear function of the number of layers, which is caused not only by the additive contribution of parallel channels of conduction through an additional layer but also by the formation of additional parallel contacts via the filling of voids in the lower layer and is consistent with previous results [15]. Several factors influence the resultant resistance of transparent conductive films based on single-walled CNTs [11]: the conductance of the starting nanotubes, the contact resistance between the nanotubes, their state of aggregation, and impurities. The conductance of the starting nanotubes is determined by both their geometric structure (semiconducting or metallic) and defects. The nanotubes used in this study were predominantly defect-free (as evidenced by the low intensity of the *D* peak in the Raman spectrum of the nanotubes in Fig. 5). Therefore, the decrease in conductance was primarily due to the random distribution of semiconducting and metallic nanotubes: in unprocessed single-walled CNTs produced by arc discharge, the fraction of semiconducting tubes exceeds 70%. In addition, the nanotubes produced by this method are typically relatively short, no longer than 1 μm , which limits their conductance because of the formation of many internanotube contacts during film growth. The conductance of nanotube films can in general be evaluated mathematically using graph theory. In the infinite nanotube approximation, the number of nodes in a graph can be found analytically and is a quadratic function of the number of tubes, which corresponds to a three-dimensional percolation of nanotubes in films [16].

Thus, it should be expected that, at a small number of layers, a slight deviation from the preset nanotube density in a network will lead to a change in resistance by several times, as evidenced by the large scatter in the resistance of five-layer films. Nevertheless, as the number of nanotube deposition cycles increases, the growth of a new layer is accompanied by a reverse process: some of the nanotubes return to the solution from

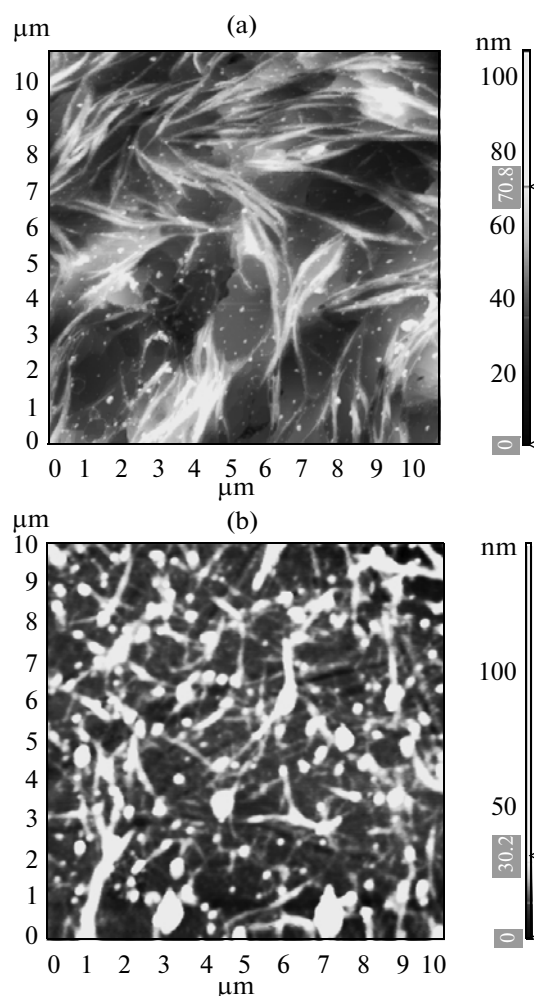


Fig. 1. Topographic images of the PEN substrate surface after CNT deposition from a surfactant solution at (a) 25 and (b) 5°C.

the substrate surface and form conglomerates with the nanotubes present in the solution. This process is promoted by the surfactant removal by rinsing in 2-propanol, which increases the coagulation rate of the nanotubes transferred to the solution from the substrate. Increased agglomeration both markedly reduces the transmittance of the films and causes the resistance of the films as a function of their thickness to deviate from inverse quadratic behavior.

Optical properties of the SWNTs. Increasing the film thickness leads not only to an increase in the conductance of the films but also to a reduction in their transmittance. Figure 4 plots the transmittance *T* of the films at an excitation wavelength $\lambda = 550$ nm against film thickness, *h*. The transmittance is seen to decrease monotonically from 85% (at a film thickness of ≈ 50 nm (five layers)) to 40% (at a film thickness of ≈ 200 nm (20 layers)). In a model for interaction of thin ($h \ll \lambda$) conductive films with light, their transmittance and thickness are related by [17]

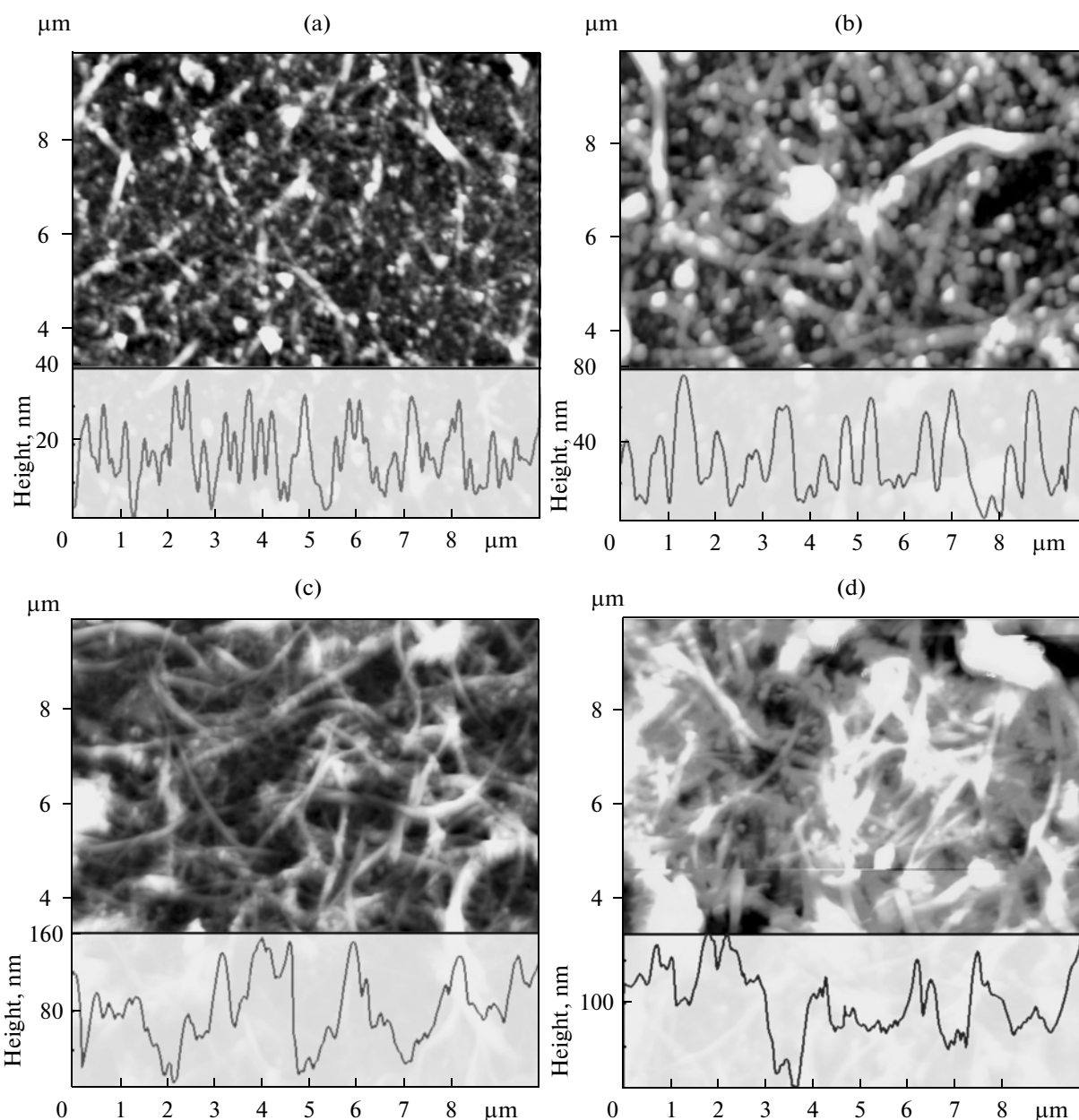


Fig. 2. AFM images of conductive nanotube films after (a) 5, (b) 10, (c) 15, and (d) 20 deposition cycles. Insets: surface height profiles of the films.

$$T(\lambda) = \frac{1}{\left(1 + \frac{Z_0}{2} \sigma_{\text{opt}}(\lambda) h\right)^2} = \frac{1}{\left(1 + \frac{Z_0}{2R_s} \frac{\sigma_{\text{opt}}(\lambda)}{\sigma_{\text{dc}}}\right)^2},$$

where Z_0 is the characteristic impedance of vacuum ($\approx 377 \Omega$), σ_{opt} is the optical conductance of the film, σ_{dc} is its dc electrical conductance, and R_s is its sheet resistance. Fitting experimental data with this relation (Fig. 4), we find the optical conductance of the films, $\sigma_{\text{opt}} = (2.9 \pm 0.4) \times 10^4 \text{ S/m}$ ($\lambda = 550 \text{ nm}$), which is a factor of 1.5–2 higher than reported previously [18, 19].

In addition, we studied the high-frequency optical properties of the films in order to assess the effect of technology on their structure. We measured the Raman spectra of all the CNT samples grown on PEN from an aqueous CTAB solution in 5, 10, 15, and 20 deposition cycles. Typical spectra are presented in Fig. 5. In the spectra of the thin films (15 layers or less), peaks from the PEN substrate are discernible: vibrations of the naphthalene rings (1390 cm^{-1}), stretching C=C vibrations of the aromatic rings (1480 and 1635 cm^{-1}), and C=O vibrations (1720 cm^{-1}) [20]. With increasing film thickness, these peaks disappear. The peaks characteristic of CTAB are an order

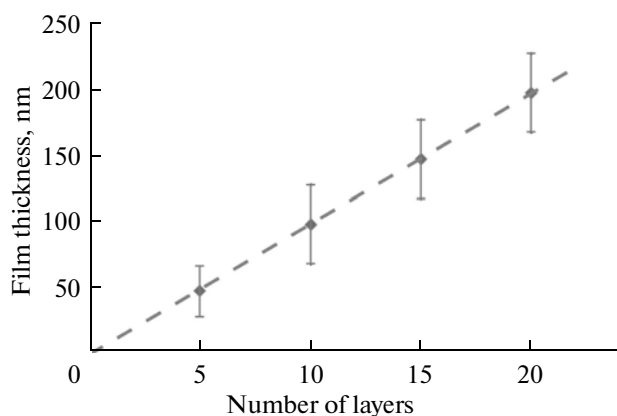


Fig. 3. Film thickness against the number of deposition cycles.

of magnitude weaker than the observed peaks of the PEN and CNTs, which is due to both the low concentration and low initial intensity of the organic material [21]. It is worth pointing out that the peaks of the PEN are not influenced by the CNTs, which suggests that there is no additional interaction between the nanotubes and substrate. At film thicknesses above 100 nm, the peaks take a shape typical of SWNTs produced by arc discharge: narrow nanotube diameter distribution (RBM) and low defect density (D) [22].

Effect of bending on the properties of the CNT films.

Figure 6 shows the resistance as a function of bend angle for a single-walled CNT film on PEN. Upon bending to the minimum radius of 3.5 mm, the resistance of the structure increases by $\approx 8\%$ when the film is under tension and decreases by $\approx 7\%$ when it is under compression. On the whole, the resistance is a linear function of bend angle, and this behavior was reproducible over more than 1000 bending/unbending cycles. The mechanism behind such reproducibility of properties can be understood in terms of displacement of the nanotubes in the plane of the substrate [23]. This may be accompanied by additional mechanical relaxation of the nanotubes on the surface through their twisting [24]. The largest changes in resistance—an increase or decrease by more than 20% relative to the initial level—were observed in cyclic measurements. One possible reason for this is that the films consist predominantly of semiconducting nanotubes, which are very sensitive to external parameters, in particular to changes in the temperature of the ambient medium during experiments.

CONCLUSIONS

We have studied the optical and electrical properties of single-walled CNT films grown through deposition from colloidal surfactant solutions at a temperature below the critical micelle temperature. Optical spectroscopy has demonstrated the possibility of obtaining transmittances in the range from 40 to 85% by varying the density and thickness of the films: with

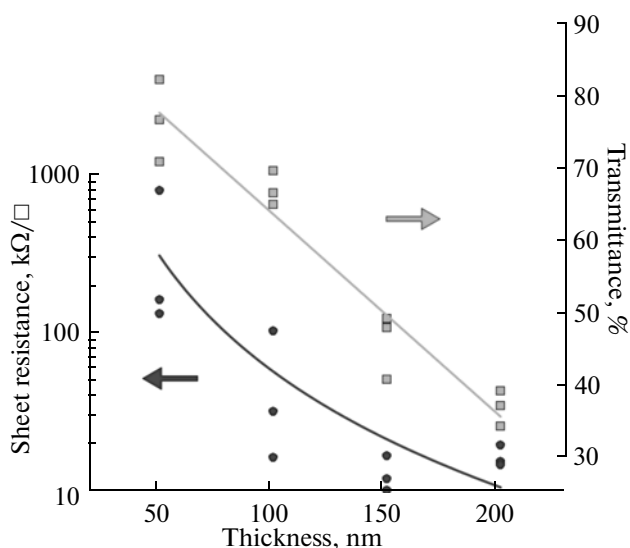


Fig. 4. Resistance and transmittance of TCFs as functions of average film thickness.

increasing density, their transmittance decreases. In the case of the densest networks, the sheet resistance of the films is several kilohms. Mechanical compression (tension) of the films upon bending to a radius of down to 3.5 mm increases (decreases) their resistance by no more than 8%. When the film is reverted back to its unstrained state, its resistance returns to its original level. Further increase in transmittance, with a decrease in resistance, can be achieved by removing impurities from the nanotubes and by using metallic nanotubes of greater length. Nevertheless, the present results demonstrate the feasibility of producing thin transparent conductive coatings on flexible substrates.

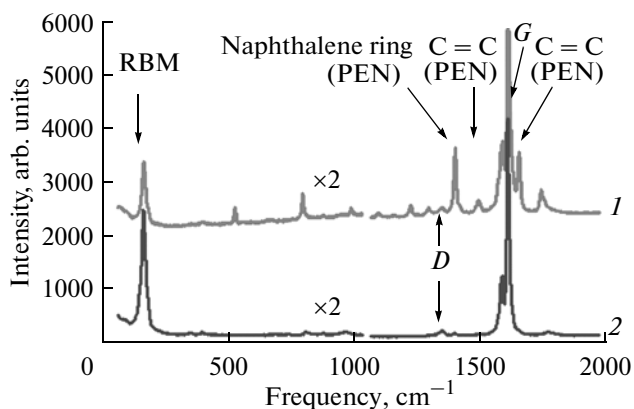


Fig. 5. Raman spectra of nanotube films after (1) 5 and (2) 20 deposition cycles. Characteristic peaks of nanotubes: RBM, radial breathing mode; D , peak due to defects in the C—C bonds; G , peak due to in-plane C—C vibrations.

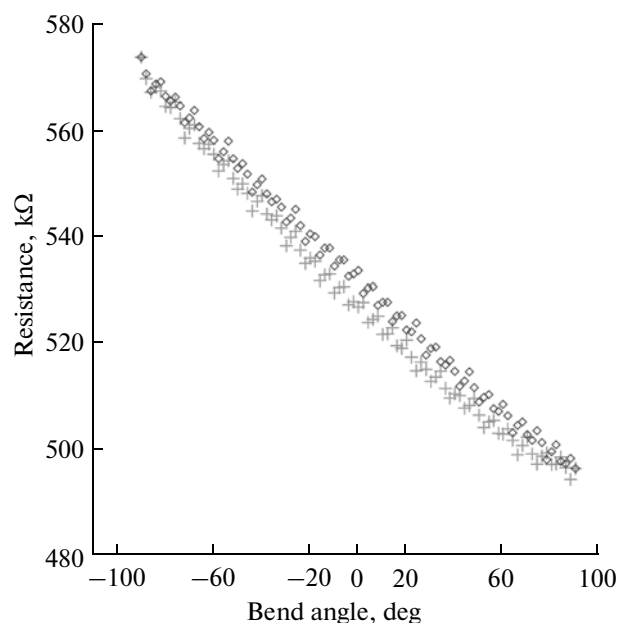


Fig. 6. Resistance as a function of bend angle for a structure with a five-layer single-walled CNT film during compression and tension. A bend angle of 90° corresponds to a radius of curvature of ≈ 3.5 mm.

ACKNOWLEDGMENTS

This work was supported by the RF Ministry of Education and Science (agreement no. 14.V37.21.0085) and the RF President's Grants Council (Support to Young Scientists Program, grant no. MD-2514.2012.8).

REFERENCES

1. Ferrer-Anglada, N., Pérez-Puigdemont, J., Figueras, J., et al., Flexible, transparent electrodes using carbon nanotubes, *Nanoscale Res. Lett.*, 2012, vol. 7, p. 571.
2. Scardaci, V., Coull, R., and Coleman, J.N., Very thin transparent, conductive carbon nanotube films on flexible substrates, *Appl. Phys. Lett.*, 2010, vol. 97, no. 2, paper 023 114.
3. Zikang, T. and Sheng, P., Nanoscale phenomena: Basic science to device applications, *Ser.: Lecture Notes Nanoscale Sci. Technol.*, 2008, vol. 2, no. 14, p. 248.
4. Han, J.T., Kim, J.S., Lee, S.G., et al., Chemical strain-relaxation of single-walled carbon nanotubes on plastic substrates for enhanced conductivity, *J. Phys. Chem. C*, 2011, vol. 115, no. 45, p. 22 251.
5. Zhang, J., Gao, L., Sun, J., et al., Dispersion of single-walled carbon nanotubes by Nafion in water/ethanol for preparing transparent conducting films, *J. Phys. Chem.*, 2008, vol. 112, p. 16 370.
6. Saran, N., Parikh, K., Suh, D.S., et al., Fabrication and characterization of thin films of single-walled carbon nanotube bundles on flexible plastic substrate, *J. Am. Chem. Soc.*, 2004, vol. 126, no. 14, p. 4462.
7. Crouzier, T., Nimmagadda, A., Nollert, M.U., and McFetridge, P.S., Modification of single walled carbon nanotube surface chemistry to improve aqueous solu-

8. Xiaolin Li, Li Zhang, Xinran Wang, et al., Langmuir-Blodgett assembly of densely aligned single-walled carbon nanotubes from bulk materials, *J. Am. Chem. Soc.*, 2007, vol. 129, no. 16. p. 4890.
9. Yan, Y.H., Chan-Park, M.B., and Zhang, Q., Advances in carbon-nanotube assembly, *Small*, 2007, vol. 3, no. 1, p. 24.
10. Pham, D.T., Subbaraman, H., Chen, M.Y., et al., Self-aligned carbon nanotube thin-film transistors on flexible substrates with novel source-drain contact and multilayer metal interconnection, *IEEE Trans. Nanotechnol.*, 2012, vol. 11, no. 1, p. 44.
11. Pei, S., Du, J., Zeng, Y., et al., The fabrication of a carbon nanotube transparent conductive film by electrophoretic deposition and hot-pressing transfer, *Nanotechnology*, 2009, vol. 20, no. 23, p. 5707.
12. Krestinin, A.V., Kiselev, N.A., Raevskii, A.V., and Rya-benko, A.G., Perspective of single-wall carbon nanotube production in the arc-discharge process, *Eurasian Chem. Tech. J.*, 2003, vol. 5, no. 1, p. 7.
13. Dan, B., Irvin, G.C., and Pasquali, M., Continuous and scalable fabrication of transparent conducting carbon nanotube films, *ACS Nano*, 2009, vol. 3, no. 4, p. 835.
14. Bobrinetskii, I.I. and Nevolin, V.K., Micromechanics of carbon nanotubes on substrates, *Mikrosist. Tekh.*, 2002, no. 4, p. 20.
15. Mandal, H.S., Ward, A., and Tang, X., Transferable thin films of pristine carbon nanotubes, *J. Nanosci. Nanotechnol.*, 2011, vol. 11, no. 4, p. 3265.
16. Hu, L., Hecht, D.S., and Gruner, G., Percolation in transparent and conducting carbon nanotube networks, *Nano Lett.*, 2004, vol. 4, no. 12, p. 2513.
17. Dressel, M. and Gruner, G., *Electrodynamics of Solids: Optical Properties of Electrons in Matter*, Cambridge: Cambridge Univ. Press, 2002.
18. Doherty, E.M., De, S., Lyons, E.P., et al., The spatial uniformity and electromechanical stability of transparent, conductive films of single walled nanotubes, *Carbon*, 2009, vol. 47, no. 10, p. 2466.
19. Zhou, Y., Hu, L., and Gruner, G., A method of printing carbon nanotube thin films, *Appl. Phys. Lett.*, 2006, vol. 88, no. 3, paper 123 109.
20. Kim, C., Cakmak, M., and Zhou, X., Effect of composition on orientation, optical and mechanical properties of bi-axially drawn pen and pen/pei blend films, *Polymer*, 1998, vol. 39, no. 10, p. 4225.
21. Borodko, Y., Jones, L., Lee, H., et al., Spectroscopic study of tetradecyltrimethylammonium bromide Pt-C14TAB nanoparticles: Structure and stability, *Langmuir*, 2009, vol. 25, no. 12, p. 6665.
22. Dresselhaus, M.S., Dresselhaus, G., Saito, R., and Jorio, A., Raman spectroscopy of carbon nanotubes, *Phys. Rep.*, 2004, vol. 409, no. 2, p. 47.
23. Wang, Y., Yang, Z., Hou, Z., et al., Flexible gas sensors with assembled carbon nanotube thin films for DMMP vapor detection, *Sens. Actuators, B*, 2010, vol. 150, no. 2, p. 708.
24. Lipomi, D.J., Vosgueritchian, M., Tee, B.C.-K., et al., Skin-like pressure and strain sensors based on transparent elastic films of carbon nanotubes, *Nat. Nanotechnol.*, 2011, vol. 6, no. 12, p. 788.

Translated by O. Tsarev